Dalton Transactions

Cite this: *Dalton Trans.*, 2012, **41**, 10784

www.rsc.org/dalton

PAPER

Prediction of 3-hydroxypyridin-4-one (HPO) log K_1 values for Fe(III)†

Yu-Lin Chen, Dave J. Barlow, Xiao-Le Kong, Yong-Min Ma and Robert C. Hider*

Received 11th June 2012, Accepted 17th July 2012
DOI: 10.1039/c2dt31254a

As a means to aid in the design of 3-hydroxypyridin-4-ones (HPOs) intended for use as therapeutic Fe^{3+} chelating agents, a novel methodology has been developed using quantum mechanical (QM) calculations for predicting the iron binding affinities of the compounds (more specifically, their log K_1 values). The reported/measured HPO log K_1 values were verified through their correlation with the corresponding sum of the compounds' ligating group pK_a values. Using a training set of eleven HPOs with known log K_1 values, reliable predictions are shown to be obtained with QM calculations using the B3LYP/6-31+G(d)/CPCM model chemistry (with Bondi radii, and water as solvent). With this methodology, the observed log K_1 values for the training set compounds are closely matched by the predicted values, with the correlation between the observed and predicted values giving $r^2 = 0.9$. Predictions subsequently made by this method for a test set of 42 HPOs of known log K_1 values gave predicted values accurate to within ±0.32 log units. In order to further investigate the predictive power of the method, four novel HPOs were synthesised and their log K_1 values were determined experimentally. Comparison of these predicted log K_1 values against the measured values gave absolute deviations of 0.22 (13.87 *vs.* 14.09), 0.02 (14.31 *vs.* 14.29), 0.12 (14.62 *vs.* 14.50), and 0.13 (15.04 *vs.* 15.17). The prediction methodology reported here is the first to be provided for predicting the absolute log K_1 values of iron-chelating agents in the absence of pK_a values.

Introduction

Iron is vital to all living organisms but becomes toxic when it saturates the natural cellular buffering mechanisms, the excess iron causing free radical formation *via* the Fenton reaction, and thereby leading to oxidative stress.[1] When there is a build-up of iron in humans – for example, in repeatedly transfused patients suffering from β-thalassaemia,[2] or sickle cell anaemia[3] – iron chelation therapy becomes necessary. The most widely used therapeutic chelator, desferioxamine (DFO)[4] is a hexadentate ligand with a very high affinity for Fe^{3+}, but it suffers the major drawback of being orally inactive. The more recently introduced synthetic alternatives, the 3-hydroxypyridin-4-ones (HPOs, Fig. 1), have also been shown to be useful therapeutic chelators, exhibiting the necessary affinity and selectivity for Fe^{3+} along with good oral activity.[5] One such compound, Deferiprone[6] (Fig. 1), has emerged as a critically important therapeutic, able to remove accumulated excess iron from the heart[7,8] and mitochondria.[9] However, the search continues for other such synthetic chelators, with the aim to develop analogues that retain the excellent iron scavenging properties of Deferiprone, but which lack this compound's relatively high metabolic instability and its undesirable effect, in a small number of patients, of lowering a patient's white blood cell count.[10]

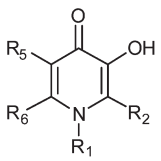

Fig. 1 3-Hydroxypyridin-4-one (HPO). Deferiprone, $R_1 = R_2 = CH_3$ and $R_5 = R_6 = H$.

The rational design of such molecules can be greatly facilitated by having accurate means to predict their affinity for Fe^{3+} and H^+ – the latter demanding an accurate means to predict the pK_a values for their iron co-ordinating moieties. In our attempts to develop such methodologies, we previously sought to explore the accuracy and reliability of the pK_a predictions that could be achieved for a series of HPOs using a number of existing, low-cost, Quantitative Structure Property Relationship (QSPR)[11,12] and Quantum Mechanical (QM)[13] methods. Using a training set of 15 HPOs with known hydroxyl pK_a values, reliable predictions were shown to be obtained with QM calculations using the B3LYP/6-31+G(d)/CPCM model chemistry (with Pauling radii, and water as solvent).[14] With this methodology, the observed hydroxyl pK_a values for the training set compounds closely

Institute of Pharmaceutical Science, King's College London, Franklin-Wilkins Building, 150 Stamford Street, London, SE1 9NH, UK. E-mail: robert.hider@kcl.ac.uk; Tel: +44 (0)20 7848 4882

†Electronic supplementary information (ESI) available. See DOI: 10.1039/c2dt31254a

matched the predicted pK_a values (with r^2 = 0.98) and the predictions subsequently made by this method for a test set of 48 HPOs of known hydroxyl pK_a values gave predicted pK_a values accurate to within ±0.2 log units.

In the studies reported here, our aim was to extend the modelling of these chelators towards prediction of their log K_1 values – hopefully, therefore, providing a rapid and reliable *in-silico* method for predicting their affinities for Fe^{3+}.

Experimental

Titrimetry

The stability constants of HPOs were determined using an automated titration system.[15] The log K_1 values were evaluated using a 10 : 1 molar ratio of Ligand (L) : Metal (Fe^{3+}). The titration data were analysed using the pHab program[16] and species plots were calculated using the HYSS program.[17]

Prediction of HPO log K_1 values using QM calculations

By analogy with a related study,[14] in order to simplify calculations and to decrease computing time, only two types of optimised structures, namely deprotonated ligand (L^-) and iron (Fe^{3+}) complex ($[Fe^{3+}L_1]^{2+}$), in solvent models were computed. The calculated free energy differences ($\Delta G^*_{calculated}$) between the two optimised structures of the starting 11 HPOs (Table 1) were plotted against their experimentally determined log K_1 values in order to assess the correlation. The correlation coefficient (r) for the regression between predicted and experimental values and their mean and standard deviation of absolute deviations ($|M|$ and $|S|$) were used to investigate the performance of various model chemistries. The different model chemistries at B3LYP/6-31+G(d) level explored here vary very significantly according to the solvent model employed[18] (IEF-PCM, CPCM, SMD, I-PCM or SCI-PCM) and the radii employed in the CPCM models (Bonding, Pauling, UFF, UAHF, or UAKS). For $[Fe^{3+}L_1]^{2+}$, there are two constructed starting structures: one, with no explicit water (Fig. 2(a)) and the other, with four explicit water molecules octahedrally distributed around the Fe^{3+} (Fig. 2(b)). All the optimised geometries (direct optimised in solvent models; force constants calculated at each step; without symmetry constraints; the spin multiplicity = 6 for $[Fe^{3+}L_1]^{2+}$) were calculated using Gaussian 09,[19] and the conformers generated verified as corresponding to local minima on their potential energy surfaces (with no imaginary frequencies existing in the output files). Prior to running the Gaussian 09 optimisation, conformational searches at AM1 level were performed using HyperChem Release 8,[20] to obtain the global (or nearly global) minimum energy conformers for all the molecules studied here. (Any further calculations including, for example, Boltzmann averaging over multiple low energy conformers were not performed since the additional computing time required could not be justified.)

The model chemistry which produced the best result was found to be B3LYP/6-31+G(d)/CPCM (Bondi radii, water as solvent) and $[Fe^{3+}L_1]^{2+}$ structures are in the absence of explicit water molecules, with r^2 = 0.90, $|M|$ = 0.16 and $|S|$ = 0.09 (Fig. 3). Adopting the same solvent model, B3LYP*/6-31+G(d) (which has 10%, 15%, 25%, 30%, 35%, or 40% Hartree–Fock exchange compared to 20% for B3LYP), CAM-B3LYP/6-31+G(d) (a modified functional which is suitable for long orbital distance calculations), B3LYP/3-21G (a lower basis set), PM6 (a semi-empirical method), were also tested. However, no superior outcomes were detected with respect to either computing accuracy or time.

Synthesis of 3-hydroxypyridin-4-ones

Synthesis of CP70

*3-Benzyloxy-6-methyl-pyran-4(1*H*)-one.*

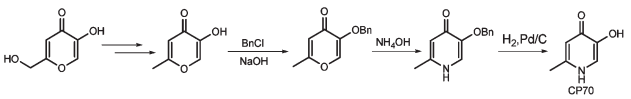

To a solution of 6-methyl-3-hydroxypyran-4(1*H*)-one (63 g, 0.5 mol) in methanol (500 mL) was added sodium hydroxide (22 g, 0.55 mol) dissolved in water (50 mL), and the mixture was heated to reflux. Benzyl chloride (70 g, 0.55 mol) was added dropwise over 30 min, and the resulting mixture was refluxed overnight. After removal of solvent by rotary evaporation, the residue was mixed with water (200 mL) and extracted with dichloromethane (3 × 150 mL). The combined extracts were washed with 5% aqueous sodium hydroxide (2 × 200 mL) followed by water (200 mL). The organic fraction was then dried over anhydrous sodium sulphate, filtered and rotary evaporated to yield an orange oil which solidified on cooling. Recrystallisation from diethyl ether affords colourless needles of the compound (88.5 g, 82%). ^{1}H NMR ($CDCl_3$): δ 2.23 (s, 3H, 6-CH_3), 5.07 (s, 2H, CH_2Ph), 6.22 (s, 1H, 5-H), 7.3-7.41 (m, 5H, Ph), 7.46 (s, 1H, 2-H).

*3-Benzyloxy-6-methyl-pyridin-4(1*H*)-one.* To a solution of 3-benzyloxy-6-methyl-pyran-4(1*H*)-one (21.6 g, 100 mmol) in a mixture of EtOH and water (200 mL; 1 : 1 v/v) was added ammonia (100 mL). The mixture was heated at 70 °C overnight. After evaporation to remove solvent, the crude product was purified by recrystallisation using EtOH–diethyl ether to afford white crystals of 3-benzyloxy-6-methyl-pyridin-4(1*H*)-one (17.4 g, 81%). ^{1}H NMR (DMSO-d_6): δ 2.16 (s, 3H, 6-CH_3), 4.97 (s, 2H, CH_2Ph), 6.01 (s, 1H, 5-H (pyridinone)), 7.31–7.41 (m, 6H, 2-H (pyridinone) and Ar), 11.15 (br., 1H, NH). MS (ESI): m/z, 216.2 $[M + H]^+$.

*3-Hydroxy-6-methyl-pyridin-4(1*H*)-one (CP70) hydrochloride.* A solution of 3-benzyloxy-6-methyl-pyridin-4(1*H*)-one (12.9 g, 60 mmol) in *N*,*N*-dimethylformamide (30 mL) was subjected to hydrogenolysis in presence of 5% Pd/C (w/w) catalyst (0.5 g) for 5 h. The catalyst was removed by filtration and the filtrate acidified to pH 1 with concentrated hydrochloric acid. After removal of the solvent *in vacuo*, the residue was purified by recrystallisation from methanol–acetone to afford a white solid (CP70) (8.6 g, 89%). ^{1}H NMR (DMSO-d_6): δ 2.49 (s, 3H, 6-CH_3), 7.13 (s, 1H, 5-H), 8.01 (s, 1H, 6-H). MS (ESI): m/z, 126.1 $[M + H]^+$. Anal.Calc. for $C_6H_7NO_2$.HCl: C, 44.60; H, 4.99; N, 8.67; Cl, 21.94%. Found C, 44.52; H, 4.75; N, 8.53; Cl, 22.05%.

Table 1 The structures, predicted (experimental) log K_1 values and calculated free energies of 3-hydroxypyridin-4-ones (HPOs)[a]

HPOs	R_1	R_2	R_5	R_6	$\Delta G^*_{calculated}$ ($G^*_{calculated}$ for $[Fe^{3+}L_1]^{2+}$, L^-) (Hartree)[c]	log K_1
CP20[b]	$-CH_3$	$-CH_3$	–H	–H	−1263.2292 (−1740.0518, −476.8226)	14.79 (15.09)[21]
CP21[b]	$-C_2H_5$	$-CH_3$	–H	–H	−1263.2305 (−1779.3418, −516.1113)	14.98 (14.82)[21]
CP23[b]	$-CH(CH_3)_2$	$-CH_3$	–H	–H	−1263.2309 (−1818.6296, −555.3987)	15.04 (15.00)[21]
CP60[b]	$-CH_3$	–H	–H	–H	−1263.2209 (−1700.7550, −437.5340)	13.64 (13.57)[21]
CP61[b]	$-C_2H_5$	–H	–H	–H	−1263.2227 (−1740.0471, −476.8244)	13.88 (14.11)[21]
CP68[b]	$-CH_3$	$-CH_3$	–H	$-CH_3$	−1263.2333 (−1779.3443, −516.1110)	15.37 (15.22)[21]
CP69[b]	$-CH_3$	–H	–H	$-CH_3$	−1263.2245 (−1740.0498, −476.8253)	14.14 (13.86)[21]
CP90[b]	–H	–H	–H	–H	−1263.2199 (−1661.4703, −398.2503)	13.50 (13.73)[21]
CP93[b]	$-CH_3$	$-C_2H_5$	–H	–H	−1263.2303 (−1779.3381, −516.1078)	14.96 (14.77)[21]
CP94[b]	$-C_2H_5$	$-C_2H_5$	–H	–H	−1263.2307 (−1818.6283, −555.3975)	15.01 (15.12)[21]
CP99[b]	–H	$-C_2H_5$	–H	–H	−1263.2282 (−1740.0596, −476.8314)	14.65 (14.82)[21]
CP360	$-CH_3$	$-CH_2OH$	–H	$-CH_3$	−1263.2241 (−1854.5518, −591.3277)	14.09 (14.39)[22]
CP369	$-C_2H_5$	$-CH_2OH$	–H	$-CH_3$	−1263.2242 (−1893.8405, −630.6162)	14.10 (14.37)[22]
CP374	$-CH_3$	$-CHC_2H_5OH$	–H	$-CH_3$	−1263.2212 (−1933.1295, −669.9084)	13.67 (14.41)[22]
CP502	$-CH_3$	$-CONHCH_3$	–H	$-CH_3$	−1263.2174 (−1948.0243, −684.8069)	13.14 (13.41)[24]
CP509	–H	$-CON(CH_3)_2$	–H	$-CH_3$	−1263.2169 (−1948.0272, −684.8103)	13.08 (12.85)[24]
CP513	$-CH_3$	$-CONHC_2H_5$	–H	$-CH_3$	−1263.2164 (−1987.3136, −724.0972)	13.00 (12.84)[24]
CP514	$-C_2H_5$	$-CONHCH_3$	–H	$-CH_3$	−1263.2183 (−1987.3120, −724.0937)	13.28 (12.96)[24]
YMF5	–H	–H	–F	–H	−1263.2103 (−1760.7086, −497.4982)	12.15 (11.57)[23]
YMF7	$-CH_3$	–F	–H	–H	−1263.2141 (−1799.9948, −536.7807)	12.69 (11.95)[23]
YMF8	$-C_2H_5$	–F	–H	–H	−1263.2146 (−1839.2858, −576.0712)	12.75 (11.98)[23]
YMF14	$-CH_3$	–F	$-CH_3$	–H	−1263.2178 (−1839.2906, −576.0728)	13.20 (13.14)[23]
YMF15	$-CH_3$	–H	–F	–H	−1263.2117 (−1799.9937, −536.7820)	12.35 (12.14)[23]
YMF16	$-C_2H_5$	–H	–F	–H	−1263.2129 (−1839.2857, −576.0728)	12.51 (12.69)[23]
YMF17	$-CH_3$	$-CH_3$	–F	–H	−1263.2196 (−1839.2903, −576.0706)	13.46 (13.61)[23]
YMF21	–H	–H	–F	$-CH_3$	−1263.2131 (−1800.0077, −536.7946)	12.54 (12.50)[23]
YMF22	–H	$-CH_3$	–F	–H	−1263.2170 (−1800.0099, −536.7929)	13.09 (13.21)[23]
YMF24	$-C_3H_7$	–F	–H	–H	−1263.2144 (−1878.5745, −615.3601)	12.73 (12.20)[23]
YMF25	$-C_3H_7$	–H	–F	–H	−1263.2124 (−1878.5741, −615.3617)	12.44 (11.88)[23]
YMF26	$-CH(CH_3)_2$	–H	–F	–H	−1263.2133 (−1878.5751, −615.3618)	12.57 (11.76)[23]
YMF33	$-C_4H_9$	–F	–H	–H	−1263.2147 (−1917.8633, −654.6486)	12.77 (12.37)[23]
CP102	$-C_2H_4OH$	$-C_2H_5$	–H	–H	−1263.2278 (−1893.8415, −630.6136)	14.61 (14.69)[d]
CP110	$-C_2H_4COOH$	$-C_2H_5$	–H	–H	−1263.2271 (−2007.2015, −743.9744)	14.50 (14.78)[d]
CP359	$-C_2H_5$	$-CH_2OH$	–H	–H	−1263.2226 (−1854.5508, −591.3281)	13.88 (14.26)[d]
CP364	$-CH_3$	$-CH_2OH$	–H	–H	−1263.2206 (−1815.2591, −552.0386)	13.59 (14.28)[d]
CP365	$-C_2H_5$	$-CHCH_3OH$	–H	–H	−1263.2197 (−1893.8404, −630.6207)	13.47 (14.15)[d]
CP366	$-C_3H_6OH$	$-CH_2OH$	–H	–H	−1263.2203 (−1969.0530, −705.8327)	13.55 (13.82)[d]
CP372	$-C_3H_6OH$	$-CHCH_3OH$	–H	–H	−1263.2195 (−2008.3458, −745.1263)	13.43 (14.29)[d]
CP511	–H	$-CONHCH_3$	–H	$-CH_3$	−1263.2063 (−1908.7534, −645.5471)	11.59 (12.03)[d]
CP545	–H	$-CONHC_2H_4OH$	–H	–H	−1263.2005 (−1983.9593, −720.7588)	10.77 (11.32)[d]
CP510	$-CH_3$	–H	–H	$-CONHCH_3$	−1263.2172 (−1908.7311, −645.5139)	13.12 (12.20)[d]
CP28	–H	$-CH_3$	–H	–H	−1263.2268 (−1700.7715, −437.5446)	14.46 (14.49)[d]
CP38	$-C_2H_4COOH$	$-CH_3$	–H	–H	−1263.2265 (−1967.9156, −704.6891)	14.42 (14.62)[d]
CP40	$-C_2H_4OH$	$-CH_3$	–H	–H	−1263.2280 (−1854.5560, −591.3280)	14.63 (14.61)[d]
CP111	$-C_3H_6COOH$	$-C_2H_5$	–H	–H	−1263.2276 (−2046.4899, −783.2623)	14.57 (14.58)[d]
CP352	$-C_2H_4OH$	$-CH(C_6H_5)OH$	–H	$-CH_3$	−1263.2162 (−2200.0370, −936.8208)	12.97 (13.02)[d]
CP362	$-CH_3$	$-CH_2OCH_3$	–H	$-CH_3$	−1263.2249 (−1893.8275, −630.6026)	14.19 (14.45)[d]
CP363	$-CH_3$	$-CH(CH_3)OCH_3$	–H	$-CH_3$	−1263.2280 (−1933.1183, −669.8903)	14.64 (15.00)[d]
CP414	$-CH_3$	$-CH_2(NC_5H_{10})$	–H	$-CH_3$	−1263.2056 (−2030.3502, −767.1446)	11.49 (11.59)[d]
CP417	$-CH_3$	$-CH_2(NC_5H_{10})$	–H	$-CH_2OH$	−1263.2013 (−2105.5593, −842.3581)	10.88 (10.98)[d]
CP751	$-CH_3$	$-CH_3$	$-CH_3$	–H	−1263.2338 (−1779.3475, −516.1137)	15.44 (15.51)[d]
YMF3	–H	–F	–F	–F	−1263.2358 (−1958.7859, −695.5501)	15.72 (15.06)[d]
YMF4	–H	–F	–H	–F	−1263.2455 (−1859.5496, −596.3041)	17.08 (16.52)[d]
CP70	–H	–H	–H	$-CH_3$	−1263.2226 (−1700.7691, −437.5465)	13.87 (14.09)[d]
CP370	$-C_2H_5$	$-CH_2OCH_3$	–H	$-CH_3$	−1263.2257 (−1933.1174, −669.8917)	14.31 (14.29)[d]
CP375	$-CH_3$	$-CHC_2H_5OCH_3$	–H	$-CH_3$	−1263.2279 (−1972.4049, −709.1770)	14.62 (14.50)[d]
CP616	–H	$-CH_3$	$-CH_3$	–H	−1263.2309 (−1740.0669, −476.8360)	15.04 (15.17)[d]

[a] Positions of substituents R_1, R_2, R_5 and R_6 (Fig. 1). [b] The first 11 HPOs were used to test different model chemistries. [c] $\Delta G^*_{calculated}$: the calculated free energy differences between $[Fe^{3+}L_1]^{2+}$ and L^- using B3LYP/6-31+G(d)/CPCM (Bondi radii, water as solvent) ($G^*_{calculated}$: the calculated free energy); 1 Hartree = 627.5095 kcal mol^{-1}. [d] The experimental values were determined in this study.

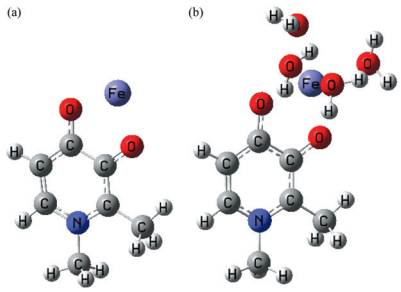

Fig. 2 $[Fe^{3+}L_1]^{2+}$ Structures: (a) without explicit water molecules; (b) with 4 explicit water molecules octahedrally distributed around Fe^{3+}.

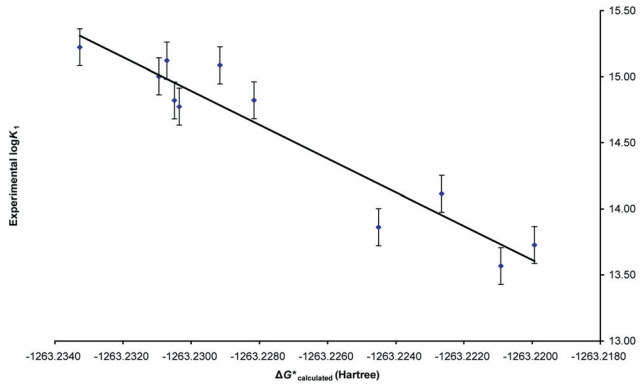

Fig. 3 The experimental log K_1 values *versus* the calculated free energy differences ($\Delta G^*_{calculated}$) for the starting 11 HPOs using B3LYP/6-31+G(d)/CPCM (Bondi radii, water as solvent). The errors related to the experimental log K_1 determination for the typical HPOs is estimated to be of the order of ±0.14 (assuming errors on the determined pK_a values of ±0.1).

Synthesis of CP370

Chlorokojic acid.

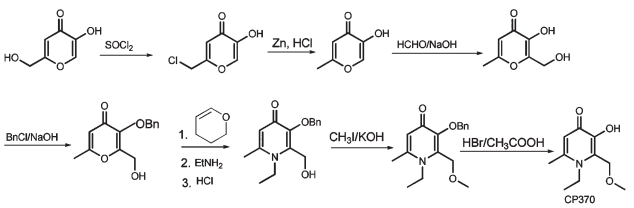

Kojic acid (200 g, 1.4 mol) was dissolved in thionyl chloride (800 mL), stirred for 1 h, after which time a yellow crystalline mass formed. The product was collected by filtration and washed with petroleum ether and then recrystallised from water to give cream coloured needles (170 g, 75.9%): ^{1}H NMR (DMSO-d_6) δ: 4.7 (s, 2H, 6-CH_2Cl), 6.6 (s, 1H, 5-H), 8.1 (s, 1H, 2-H), 9.3 (br., s, 1H, 3-OH).

*6-Methyl-3-hydroxypyran-4(1*H*)-one.* Chlorokojic acid (150 g, 0.94 mol) was added to 500 mL of distilled water and heated to 50 °C with stirring. Zinc dust (122 g, 1.88 mol) was added followed by the dropwise addition of concentrated hydrochloric acid (280 mL) over 1 h with vigorous stirring maintaining the temperature between 70–80 °C. The reaction mixture was stirred for a further 3 h at 70 °C. Excess zinc was removed by hot filtration and the filtrate extracted with dichloromethane (10 × 200 mL). The combined organic extracts were dried, filtered and concentrated *in vacuo* to yield the crude product. Recrystallisation from isopropanol afforded straw coloured plates (70 g, 60.8%): ^{1}H NMR (DMSO-d_6): δ 2.25 (s, 3H, 6-CH_3), 6.2 (s, 1H, 5-H), 6.3–7.35 (br., 1H, 3-OH), 7.7 (s, 1H, 2-H).

*2-Hydroxymethyl-3-hydroxy-6-methyl-pyran-4(1*H*)-one.* 6-Methyl-3-hydroxypyran-4(1*H*)-one (68 g, 540 mmol) was added to an aqueous solution of sodium hydroxide (23.7 g, 594 mmol) in distilled water (500 mL) and stirred at room temperature for 5 min. 35% Formaldehyde solution (49 mL) was added dropwise over 10 min and the solution allowed to stir for 12 h. Acidification to pH 1 using concentrated hydrochloric acid and cooling to 3–5 °C for 12 h gave a crystalline deposit (65 g, 75%), ^{1}H NMR (DMSO-d_6): δ 2.3 (s, 3H, 6-CH_3), 4.5 (s, 2H, 2-CH_2OH), 4.6–5.7 (br., 1H, 2-CH_2OH), 6.25 (s, 1H, 5-H), 8.7–9.2 (br., 1H, 3-OH).

*2-Hydroxymethyl-3-benzyloxy-6-methyl-pyran-4(1*H*)-one.* Sodium hydroxide (17.7 g, 434 mmol, 1.1 equiv) dissolved in 37 mL distilled water was added to a solution of 2-hydroxymethyl-3-hydroxy-6-methyl-pyran-4(1*H*)-one (63 g, 403 mmol, 1 equiv) in methanol (367 mL) and the reaction mixture was heated to reflux. Benzyl chloride (76 g, 403 mmol, 1 equiv) was added dropwise over 30 min and then refluxed for 12 h. The reaction mixture was concentrated *in vacuo*, the residue taken up into dichloromethane (1 L) and the inorganic salts filtered off. The dichloromethane layer was washed with 5% sodium hydroxide solution (6 × 100 mL), water (600 mL), dried, filtered and concentrated *in vacuo* to yield the crude product as a yellow crystalline solid. Recrystallisation from dichloromethane–petroleum ether 40 : 60 afforded a white crystalline solid (70 g, 71%): ^{1}H NMR ($CDCl_3$): δ 2.2 (s, 3H, 6-CH_3), 2.6 (br., s, 1H, 2-*CH_2*OH), 4.3 (br., s, 2H, 2-CH_2*OH*), 5.2 (s, 2H, CH_2Ph), 6.15 (s, 1H, 5-H (pyranone)), 7.4–7.6 (m, 5H, Ar).

*3-Benzyloxy-1-ethyl-2-hydroxymethyl-6-methyl-1*H*-pyridin-4(1*H*)-one.* To a solution of 2-hydroxymethyl-3-benzyloxy-6-methyl-pyran-4(1*H*)-one (68 g, 277 mmol, 1 equiv) in dichloromethane (830 mL) was added 3,4-dihydro-2*H*-pyran (47 g, 554 mmol, 2 equiv) followed by *p*-toluenesulfonic acid monohydrate (800 mg, cat.). After being stirred at room temperature for 3 h, the reaction mixture was washed with 5% aqueous sodium carbonate (500 mL) followed by water (4 × 250 mL). The organic fraction was then dried, filtered, and rotary evaporated to yield a light yellow oil. This oil was dissolved in ethanol (280 mL)/aqueous ethylamine (280 mL) and refluxed at 70 °C for 12 h. After removal of the solvent by rotary evaporation, the residue was re-dissolved in ethanol (200 mL) and 2 N hydrochloric acid (140 mL) and refluxed for 4 h. The solvent was removed by rotary evaporation prior to addition of water (140 mL) and washing with diethyl ether (2 × 300 mL). Subsequent adjustment of the aqueous fraction to pH 9 with 10 N sodium hydroxide solution was followed by extraction into dichloromethane (4 × 300 mL), the combined organic layers were dried, filtered, and rotary evaporated to give a light brown solid. Crystallisation from methanol–diethyl ether afforded the pure product (44 g, 75%) as a creamy white crystalline solid. ^{1}H NMR (DMSO-d_6): δ 1.21–1.24 (t, 3H, J = 7.15 Hz, CH_3, N-Et), 2.35 (s, 3H, 6-CH_3), 4.06–4.12 (q, 2H, J = 7.13 Hz, CH_2, N-Et), 4.6 (s, 2H, 2-*CH_2*OH), 5.05 (s, 2H, *CH_2*Ph), 6.16 (s, 1H, 5-H), 7.4–7.6 (m, 5H, Ar).

3-Benzyloxy-1-ethyl-2-methoxymethyl-6-methyl-pyridin-4(1H)-one. To DMSO (30 mL) was added 3-benzyloxy-1-ethyl-2-hydroxymethyl-6-methyl-pyridin-4(1*H*)-one (1 g, 3.66 mmol, 1 equiv) and stirred, until completely dissolved. This solution was added to KOH (411 mg, 7.32 M, 2 equiv) and stirred for another 3 h. The above reaction vessel was sealed and iodomethane (2.6 g, 18.3 mmol, 5 equiv) was injected dropwise over 10 min and allowed to stir overnight. A reddish brown clear mixture was obtained at the end of the period. The reaction mixture was reduced under pressure and the contents taken up in 500 mL water.

The aqueous layer was extracted with DCM (5 × 100 mL), the combined extracts dried, filtered and dried to obtain the crude product as yellow oil. Column chromatography using MeOH–$CHCl_3$ = 1 : 9 yielded the pure compound as a white solid (900 mg, 95%). ^{1}H NMR ($CDCl_3$): δ 1.23–1.26 (t, 3H, J = 7.15 Hz, CH_3), 2.35 (s, 3H, 6-CH_3), 3.23 (s, 3H, OCH_3), 4.00–4.05 (q, 2H, J = 7.13 Hz, CH_2), 4.37 (s, 2H, CH_2OCH_3), 5.24 (s, 2H, CH_2Ph), 6.4 (s, 1H, 5-H (pyridinone)), 7.4–7.6 (m, 5H, Ar).

1-Ethyl-3-hydroxy-2-methoxymethyl-6-methyl-pyridin-4(1H)-one (CP370). To a solution of 3-benzyloxy-1-ethyl-2-methoxymethyl-6-methyl-pyridin-4(1*H*)-one (800 mg, 2.78 mmol) in DCM (10 mL) in a sealed container was added 6 mL of 33% HBr in acetic acid and left to stir for 2 h. At the end of the period diethyl ether was added to the reaction mixture to precipitate the product. The crude off-white solid was filtered, dried and then recrystallised from methanol and diethyl ether to yield pure white crystals (250 mg, 50%). ^{1}H NMR (DMSO-d_6): δ 1.35–1.39 (t, 3H, J = 7.15 Hz, CH_3), 2.64 (s, 3H, 6-CH_3), 3.34 (s, 3H, OCH_3), 4.35–4.40 (q, 2H, J = 7.13 Hz, CH_2), 4.73 (s, 2H, CH_2OCH_3), 7.08 (s, 1H, 5-H). MS (ESI): m/z, 198.1 $[M + H]^+$. Anal.Calc. for $C_{10}H_{15}NO_3$. HBr: C, 43.18; H, 5.80; N, 5.04; Br, 28.73%. Found C, 43.11; H, 5.59; N, 4.9; Br, 28.78%.

Synthesis of CP375

2-(1′-Hydroxypropyl)-3-hydroxy-6-methyl-pyran-4(1H)-one.

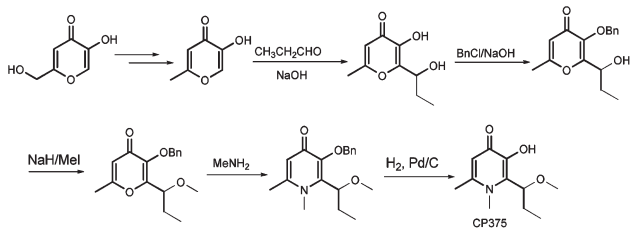

6-Methyl-3-hydroxypyran-4(1*H*)-one (12.6 g, 100 mmol) was added to 100 mL water and the pH of the solution was adjusted to 10.5 using aqueous sodium hydroxide (10 M). The mixture was stirred at room temperature for 5 min. Propionaldehyde (8.7 g, 150 mmol) dissolved in 50 mL methanol was added dropwise over 1 h and the solution allowed to stir at room temperature for 2 days. After adjustment to pH 1 with concentrated hydrochloric acid, the reaction mixture was evaporated to dryness and the residue taken up into 300 mL of dichloromethane. The organic layer was washed with water (150 mL), dried over anhydrous sodium sulphate, filtered and concentrated to yield the crude product. Recrystallisation from toluene afforded the pure product as a white crystalline solid. ^{1}H NMR ($CDCl_3$): δ 1.12 (t, 3H, J = 7.2 Hz, 2-$CHCH_2CH_3$), 1.7–2.3 (m, 2H, 2-$CHCH_2CH_3$), 2.45 (s, 3H, 6-CH_3), 4.95 (t, 1H, J = 6.0 Hz, 2-$CHCH_2CH_3$), 5.0–6.0 (br, 1H, 2-CH*OH*), 6.3 (s, 1H, 5-H).

2-(1′-Hydroxypropyl)-3-benzyloxy-6-methyl-pyran-4(1H)-one. To a solution of 2-(1′-hydroxypropyl)-3-hydroxy-6-methyl-pyran-4(1*H*)-one (7.36 g, 40 mmol) in methanol (50 mL) was added sodium hydroxide (1.76 g, 44 mmol) dissolved in water (5 mL), and the mixture was heated to reflux. Benzyl chloride (5.6 g, 44 mmol) was added dropwise over 30 min, and the resulting mixture was refluxed overnight. After removal of solvent by rotary evaporation, the residue was mixed with water (50 mL) and extracted with dichloromethane (3 × 50 mL). The combined extracts were washed with 5% aqueous sodium hydroxide (2 × 50 mL) followed by water (50 mL). The organic fraction was then dried over anhydrous sodium sulphate, filtered and rotary evaporated to yield a crude product as a yellow crystalline solid. Recrystallisation from dichloromethane–petroleum ether 40 : 60 affords colourless needles (8.9 g, 81%). ^{1}H NMR ($CDCl_3$): δ 0.8 (t, 3H, J = 7.2 Hz, 2-$CHCH_2CH_3$), 1.2–1.9 (m, 2H, 2-$CHCH_2CH_3$), 2.2 (s, 3H, 6-CH_3), 2.4 (br., s, 1H, 2-CH*OH*), 4.5 (t, J = 6.2 Hz, 1H, 2-$CHCH_2CH_3$), 5.08 (s, 2H, CH_2Ph), 6.04 (s, 1H, 5-H), 7.28 (s, 5H, Ph).

2-(1′-Methoxypropyl)-3-benzyloxy-6-methyl-pyran-4(1H)-one. To a suspension of sodium hydride (0.96 g, 40 mmol) in 50 mL dry DMF was added 2-(1′-hydroxypropyl)-3-benzyloxy-6-methyl-pyran-4(1*H*)-one (5.48 g, 20 mmol) followed by dropwise addition of iodomethane (8.52 g, 60 mmol) at 0 °C under nitrogen. After stirring for 30 min at this temperature, the reaction mixture was poured into ice cold water (100 mL) and extracted with dichloromethane (3 × 50 mL). The combined organic fractions were dried over anhydrous sodium sulphate, filtered and concentrated *in vacuo* to yield the crude product (5.2 g, 90%) as an orange oil which solidified on cooling. Recrystallisation from CH_2Cl_2–petroleum ether 40 : 60 afforded the pure product as a white crystalline solid. ^{1}H NMR ($CDCl_3$): δ 0.9 (t, 3H, J = 7.2 Hz, 2-$CHCH_2CH_3$), 1.2–1.8 (m, 2H, 2-$CHCH_2CH_3$), 2.34 (s, 3H, 6-CH_3), 3.18 (s, 3H, OCH_3), 4.3 (t, J = 6.2 Hz, 1H, 2-$CHCH_2CH_3$), 5.24 (s, 2H, CH_2Ph), 6.2 (s, 1H, 5-H), 7.38 (s, 5H, Ph).

1,6-Dimethyl-2-(1′-methoxypropyl)-3-benzyloxypyridin-4(1H)-one. To a solution of 2-(1′-methoxypropyl)-3-benzyloxy-6-methyl-pyran-4(1*H*)-one (4.32 g, 15 mmol) in EtOH (10 mL)/water (10 mL) was added 3.49 g (45 mmol) of 40% aqueous methylamine followed by 2 N sodium hydroxide solution until pH 13 was obtained. The reaction mixture was sealed in a thick-walled glass tube and stirred at 70 °C overnight. After adjustment to pH 1 with concentrated HCl, the solvent was removed by rotary evaporation prior to addition of water (50 mL) and washing with diethyl ether (3 × 50 mL). Subsequent adjustment of the aqueous fraction to pH 7 with 10 N sodium hydroxide solution was followed by extraction into dichloromethane (4 × 50 mL). The combined organic fractions were dried over anhydrous sodium sulphate, filtered and concentrated *in vacuo*. The residue was purified by column chromatography on silica gel (eluent: 15% MeOH/85% $CHCl_3$) to yield the title compound as a yellow oil (1.7 g, 38%). ^{1}H NMR ($CDCl_3$): δ 0.9 (t, 3H, J = 7.2 Hz, 2-$CHCH_2CH_3$), 1.1–1.9 (m, 2H, 2-$CHCH_2CH_3$), 2.3 (s, 3H, 6-CH_3), 3.05 (s, 3H, OCH_3), 3.65 (s, 3H, NCH_3),

4.65–5.0 (t, J = 5.4 Hz, 1H, 2-CHCH$_2$CH$_3$), 5.24 (s, 2H, CH_2Ph), 6.3 (s, 1H, 5-H), 7.1–7.6 (s, 5H, Ph).

*1,6-Dimethyl-2-(1′-methoxypropyl)-3-hydroxypyridin-4(1*H*)-one (CP375) hydrochloride.* 1,6-Dimethyl-2-(1′-methoxypropyl)-3-benzyloxypyridin-4(1*H*)-one (1.65 g, 5.5 mmol) was dissolved in MeOH (10 mL)/water (10 mL) and adjusted to pH 1 with concentrated HCl prior to hydrogenolysis for 4 h in the presence of 5% Pd/C catalyst (0.35 g). Filtration followed by rotary evaporation gave the crude product as a white solid. Recrystallisation from ethanol–diethyl ether gave the pure title compound as a white crystalline solid (1.08 g, 79%). ^{1}H NMR (DMSO-d$_6$): δ 0.9 (t, 3H, J = 7.2 Hz, 2-CHCH$_2$$CH_3$), 1.4–2.3 (m, 2H, 2-CH$CH_2CH_3$), 2.6 (s, 3H, 6-CH$_3$), 3.28 (s, 3H, OCH$_3$), 4.04 (s, 3H, NCH$_3$), 5.15 (t, J = 5.8 Hz, 1H, 2-CHCH$_2$CH$_3$), 7.4 (s, 1H, 5-H). MS (ESI): m/z, 212.1 [M + H]$^+$. Anal.Calc. for C$_{11}$H$_{18}$NO$_3$Cl: C, 53.33; H, 7.32; N, 5.65. Found: C, 53.30; H, 7.18; N, 5.56%.

Synthesis of CP616

*2-Methyl-3-benzyloxypyran-4(1*H*)-one.*

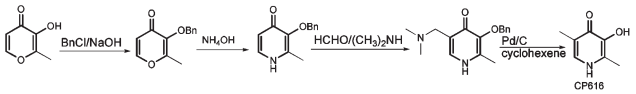

To a solution of maltol (63 g, 0.5 mol) in methanol (500 mL) was added sodium hydroxide (22 g, 0.55 mol) dissolved in water (50 mL), and the mixture was heated to reflux. Benzyl chloride (70 g, 0.55 mol) was added dropwise over 30 min, and the resulting mixture was refluxed overnight. After removal of solvent by rotary evaporation, the residue was mixed with water (200 mL) and extracted with dichloromethane (3 × 150 mL). The combined extracts were washed with 5% aqueous sodium hydroxide (2 × 200 mL) followed by water (200 mL). The organic fraction was then dried over anhydrous sodium sulphate, filtered and rotary evaporated to yield an orange oil which solidified on cooling. Recrystallisation from diethyl ether gave white needles (87.5 g, 81%). ^{1}H-NMR (CDCl$_3$): 2.12 (s, 3H, CH$_3$), 5.11 (s, 2H, CH$_2$), 6.25 (d, J = 6 Hz, 1H, 5-H), 7.28 (s, 5H, Ph), 7.47 (d, J = 6 Hz, 1H, 6-H).

*2-Methyl-3-benzyloxypyridin-4(1*H*)-one.* To a solution of 2-methyl-3-benzyloxypyran-4(1*H*)-one (13.8 g, 64 mmol) in ethanol (25 mL) was added ammonia solution (50 mL) and refluxed overnight. The solvent was removed under reduced pressure, then taken into water and adjusted to pH 1 with concentrated hydrochloric acid. The aqueous mixture was washed with ethyl acetate (3×) and the pH was adjusted to pH 10 with sodium hydroxide (2 M). The aqueous phase was extracted with chloroform (3×), dried over anhydrous sodium sulfate, filtered, and evaporated under reduced pressure. Recrystallisation from methanol–diethyl ether gave brown cubic crystals (75%). ^{1}H NMR (CDCl$_3$) δ 2.15 (3H, s, CH$_3$), 5.03 (2H, s, CH$_2$), 6.35 (1H, d, J = 6.9 Hz, 5-H), 7.25–7.31 (5H, m, Ph), 7.39 (1H, d, J = 6.9 Hz, 6-H); MS (ES): m/z, 215.1 [M + H]$^+$.

*3-Benzyloxy-5-(dimethylaminomethyl)-2-methyl-4(1*H*)-pyridinone.* To a mixture of dimethylamine (1.80 g, 40 mmol) and 40% formaldehyde (1.5 g, 20 mmol) in ethanol (100 mL) was added 3-benzyloxy-2-methyl-4(1*H*)-pyridinone (2.15 g, 10 mmol). The mixture was refluxed for 24 h and followed by rotary evaporation to afford an oil, which was crystallised after cooling. The crude product was recrystallised from ethanol–acetone to afford colourless solid (2.58 g, 95%). ^{1}H NMR (DMSO-d$_6$): 2.07 (s, 3H, CH$_3$), 2.15 (s, 6H, N(CH$_3$)$_2$), 3.25 (s, 2H, NCH$_2$), 5.03 (s, 2H, OCH$_2$), 7.28–7.41 (m, 6H, 6-H and Ph). MS (ES): m/z, 273.2 [M + H]$^+$.

*2,5-Dimethyl-3-hydroxy-4(1*H*)-pyridinone (CP616).* To a solution of 3-benzyloxy-5-(dimethylaminomethyl)-2-methyl-4(1*H*)-pyridinone (1.36 g. 5 mmol) in anhydrous ethanol (30 mL) was added cyclohexene (40 mL) and palladium hydroxide on carbon (1 g). The mixture was refluxed for 4 days with further additions of cyclohexene (40 mL) and palladium hydroxide (1.5 g) at intervals and then cooled. The precipitate was removed by filtration and resuspended in ethanol, filtered twice to recover product and the combined filtrates were evaporated to dryness under vacuum. The crude solid was recrystallised from acetone–ethanol to afford white solid (87%). ^{1}H NMR (DMSO-d$_6$): 1.92 (s, 3H, 5-CH$_3$), 2.18 (s, 3H, 2-CH$_3$), 7.38 (s, 1H, 6-H). MS (ES): m/z, 140.1 [M + H]$^+$. Anal.Calc. for C$_7$H$_9$NO$_2$: C, 60.42; H, 6.52; N, 10.07. Found: C, 60.38; H, 6.39; N, 10.01%.

Results

Validation of experimental log K_1 values

In order to obtain a large group of HPOs with reliable experimentally determined log K_1 values, a plot of log K_1 value *versus* the corresponding sum of pK_a values (hydroxyl pK_a values plus carbonyl pK_a values) was utilised. From the existing literature,[21–25] 41 HPOs were selected for initial analysis. Thirty one of these HPOs were found to give the expected linear correlation[26] between their log K_1 values and the corresponding sum of their pK_a values, r^2 = 0.95 (Fig. 4). However, 9 HPOs were found to have significantly higher log K_1 values than predicted from the linear relationship, while 1 HPO was found to possess a significantly lower log K_1 value (Fig. 4). After determining the affinity constants using a 10 : 1 molar ratio of L : Fe^{3+} for the 10 HPO outliers (Table 1; Table S1 in ESI,† including former values) and 16 previously uncharacterised HPOs (Table 1), 4 of which were specifically synthesised for this study, 57 HPOs in total were found to give the expected linear relationship between

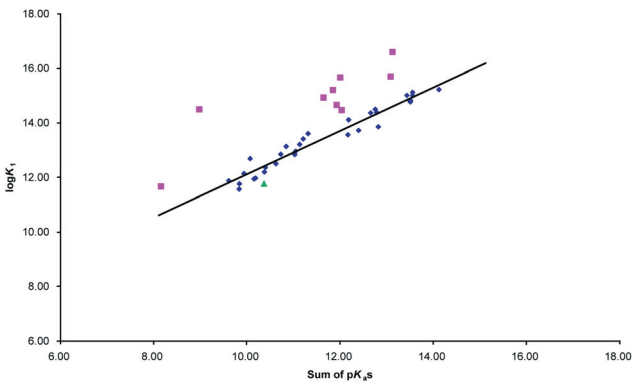

Fig. 4 log K_1 values *versus* sum of pK_a values for 41 HPOs[a], extracted from the existing literature.[21–25] ■ CP102, CP110, CP359, CP364, CP365, CP366, CP372, CP511, CP545. ▲ CP510; [a]the structures of the 41 HPOs are presented in the first 41 rows of Table 1.

their log K_1 values and the corresponding sum of pK_a values, $r^2 = 0.95$ (Fig. 5).

Experimental log K_1 determination

The UV/Vis spectra and a species plot of CP511 with a 10 : 1 molar ratio of L : Fe^{3+} are presented in Fig. 6. Two isosbestic points occur in the spectral series resulting from titration with Fe^{3+}; one at λ 600 nm, corresponding to the formation of $[Fe^{3+}(CP511)_2]^+$ and the other at λ 504 nm, corresponding to the formation of $[Fe^{3+}(CP511)_3]$. The speciation plot demonstrates that $[Fe^{3+}(CP511)_1]^{2+}$ dominates in solution from pH 0.5 to pH 1; $[Fe^{3+}(CP511)_2]^+$ dominates in solution from pH 1.5 to pH 2 and $[Fe^{3+}(CP511)_3]$ dominates in solution from pH 3 through to pH 10. The log K_1 value (12.03) was determined from curve fitting analysis of the spectra. Members of entire HPO series have similar UV/Vis spectra for their $[Fe^{3+}L_1]^{2+}$, $[Fe^{3+}L_2]^+$ and $[Fe^{3+}L_3]$ species. The log K_1 values of 26 HPOs, 4 of which were specifically synthesised for this study, were determined using this methodology (Table 1).

Development of a log K_1 prediction model

As discussed above, B3LYP/6-31+G(d)/CPCM (Bondi radii, water as solvent), with $[Fe^{3+}L_1]^{2+}$ structures being in the absence of explicit water molecules, was found to produce a relatively reliable prediction of log K_1 values for an initial series of eleven HPOs. The log K_1 values for an additional 42 HPOs were calculated using the same model chemistry to develop the final log K_1 prediction model – Predicted log $K_1 = -140.18\Delta G^*_{calculated} - 177063.32$ ($r^2 = 0.90$, $|M| = 0.32$ and $|S| = 0.25$, Fig. 7; values in Table 1). In an attempt to further examine the predictive power of this model, four novel HPOs, CP70, CP370, CP375 and CP616, were synthesised. The predicted values of all four compounds were observed to be close to their experimental values, indicating reliable predictions (Fig. 7). The absolute deviations between the predicted and experimental values are 0.22 for CP70 (13.87 *vs.* 14.09), 0.02 for CP370 (14.31 *vs.* 14.29), 0.12 for CP375 (14.62 *vs.* 14.50), and 0.13 for CP616 (15.04 *vs.* 15.17).

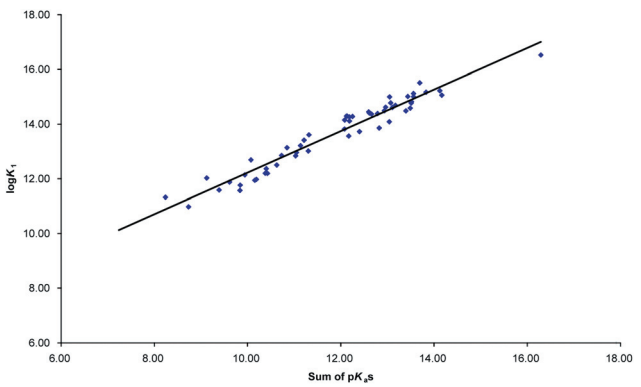

Fig. 5 log K_1 values *versus* sum of pK_a values for 57 HPOs. The structures of the 57 HPOs are presented in Table 1.

Discussion

The methodology developed for prediction of HPO log K_1 values is impressive (with the observed and predicted values strongly correlated, with r^2 of 0.9; Fig. 7). In comparison, the errors associated with the experimental determination of log K_1 for the typical HPOs is estimated to be of the order of

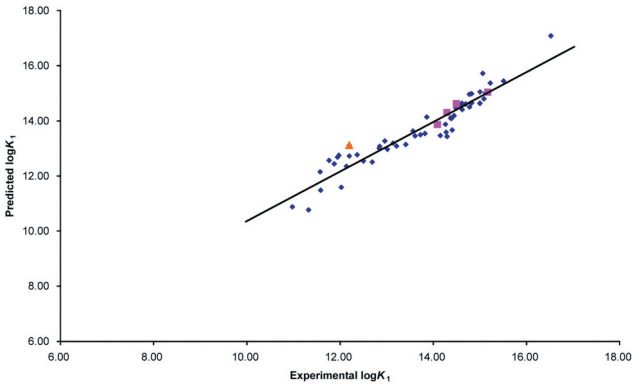

Fig. 7 Developed log K_1 prediction model. ■ CP70, CP370, CP375 and CP616; ▲ CP510 with the largest absolute deviation (0.92). Omission of the CP510 data point changes only the third decimal place in r^2 and results in an insignificant change of the fitted line, and thus an insignificant change of the predicted log K_1 values.

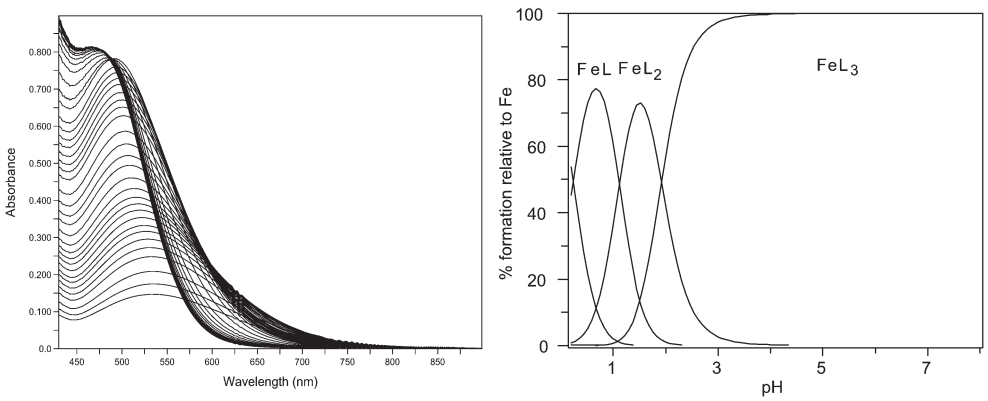

Fig. 6 The UV/Vis spectra and species plot of CP511-iron(III) for log K_1 determination when [CP511] = 445.4 μM and [Fe^{3+}] = 44.2 μM.

±0.14 (assuming errors on the determined pK_a values of ±0.1). However, for some HPOs which are associated with experimentally difficult log K_1 determinations, the error can exceed 1.0 (Table S1 in ESI†). The plot of log K_1 *versus* the corresponding sum of pK_a values (Fig. 5) was utilised to evaluate this experimental error. The utilisation of the sum of pK_a values rather than the single carbonyl or hydroxyl pK_a value was adopted because both of the pK_a values are associated with functional groups which coordinate Fe^{3+}.

The 10 HPO outliers in Fig. 4 can be categorised into 4 main subclasses, namely 1-hydrogen-(2 or 6)-amido-, 2-hydroxymethyl-, 1-hydroxy(ethyl or propyl)- and 1-carboxyethyl-HPOs. All these HPOs possess hydrogen bonding donors and acceptors on the aromatic ring substituents and this may result in a disturbance of the first layer of solvation molecules surrounding each iron (Fe^{3+}) complex. This in turn will influence the magnitudes of their stability constants; for instance, with CP511, which has strong intramolecular hydrogen bonding,[24] there is an appreciable decrease in log K_1 values (Fig. S1 in ESI†) when increased molar ratios of L : Fe^{3+} are employed in the titration. This effect is probably associated with the partial formation of a μ-oxo bridge species (Fe^{3+}–O–$Fe^{3+}L^{-}_1$) at relatively high Fe^{3+} molar concentrations, thus disturbing the UV/Vis spectra. For this reason, the 10 : 1 molar ratio of L : Fe^{3+} was adopted to minimise the formation of μ-oxo bridges during the experimental determination of log K_1 values in this study.

A knowledge of pK_a values can be neglected using the developed prediction methodology for HPO log K_1 values and this is particularly useful to predict HPOs possessing at least three pK_a values. For the experimental log K_1 determination of HPOs with more than two pK_a values, special attention is required to identify which two pK_a values correspond to the iron-coordinating oxygens. If the two pK_a values are incorrectly assigned, there will be an appreciable error in the associated experimental log K_1 value.

In summary, the methodology developed in this study is the first quantum mechanical approach to predict the absolute log K_1 value of iron-chelating agents in the absence of pK_a values. The plot of log K_1 values *versus* the corresponding sum of pK_a values (of co-ordinating atoms) has proved to be extremely useful in order to investigate the accuracy of experimentally determined log K_1 values. The stability constants for HPOs with substituents possessing hydrogen bonding donors and acceptors should be determined using a 10 : 1 molar ratio of L : Fe^{3+}.

References

1 O. Weinreb, T. Amit, S. Mandel, L. Kupershmidt and M. B. Youdim, *Antioxid. Redox Signaling*, 2010, **13**, 919–949.
2 E. J. Neufeld, *Blood*, 2006, **107**, 3436–3441.
3 W. Hagar and E. Vichinsky, *Br. J. Haematol.*, 2008, **141**, 346–356.
4 H. Keberle, *Ann. N. Y. Acad. Sci.*, 1964, **119**, 758–768.
5 T. Zhou, Y. Ma, X. Kong and R. C. Hider, *Dalton Trans.*, 2012, **41**, 6371–6389.
6 E. R. Huehns, J. B. Porter and R. C. Hider, *Hemoglobin*, 1988, **12**, 593–600.
7 C. Borgna-Pignatti, M. D. Cappellini, P. De Stefano, G. C. Del Vecchio, G. L. Forni, M. R. Gamberini, R. Ghilardi, A. Piga, M. A. Romeo, H. Zhao and A. Cnaan, *Blood*, 2006, **107**, 3733–3737.
8 A. Pepe, A. Meloni, M. Capra, P. Cianciulli, L. Prossomariti, C. Malaventura, M. C. Putti, A. Lippi, M. A. Romeo, M. G. Bisconte, A. Filosa, V. Caruso, A. Quarta, L. Pitrolo, M. Missere, M. Midiri, G. Rossi, V. Positano, M. Lombardi and A. Maggio, *Haematologica*, 2010, **96**, 41–47.
9 O. Kakhlon, H. Manning, W. Breuer, N. Melamed-Book, C. Lu, G. Cortopassi, A. Munnich and Z. I. Cabantchik, *Blood*, 2008, **112**, 5219–5227.
10 A. R. Cohen, R. Galanello, A. Piga, V. De Sanctis and F. Tricta, *Blood*, 2003, **102**, 1583–1587.
11 *ACD/pKa DB 12.0*, http://www.acdlabs.com/ (assessed February, 2011).
12 *Marvin 5.4.0.1*, http://www.chemaxon.com/ (assessed February, 2011).
13 J. Ho and M. Coote, *Theor. Chem. Acc.: Theory, Computation, and Modeling (Theoretica Chimica Acta)*, 2010, **125**, 3–21.
14 Y. L. Chen, D. J. Barlow, X. L. Kong, Y. M. Ma and R. C. Hider, *Dalton Trans.*, 2012, **41**, 6549–6557.
15 X. L. Kong, T. Zhou, H. Neubert, Z. D. Liu and R. C. Hider, *J. Med. Chem.*, 2006, **49**, 3028–3031.
16 P. Gans, A. Sabatini and A. Vacca, *Ann. Chim. (Rome, Italy)*, 1999, **89**, 45–49.
17 L. Alderighi, P. Gans, A. Ienco, D. Peters, A. Sabatini and A. Vacca, *Coord. Chem. Rev.*, 1999, **184**, 311–318.
18 J. B. Foresman and Æ. Frisch, *Exploring Chemistry with Electronic Structure Methods*, Gaussian, Pittsburgh, PA, 2nd edn, 1996.
19 M. J. Frisch, G. W. Trucks, H. B. Schlegel, G. E. Scuseria, M. A. Robb, J. R. Cheeseman, G. Scalmani, V. Barone, B. Mennucci, G. A. Petersson, H. Nakatsuji, M. Caricato, X. Li, H. P. Hratchian, A. F. Izmaylov, J. Bloino, G. Zheng, J. L. Sonnenberg, M. Hada, M. Ehara, K. Toyota, R. Fukuda, J. Hasegawa, M. Ishida, T. Nakajima, Y. Honda, O. Kitao, H. Nakai, T. Vreven, J. Montgomery Jr., J. E. Peralta, F. Ogliaro, M. Bearpark, J. J. Heyd, E. Brothers, K. N. Kudin, V. N. Staroverov, R. Kobayashi, J. Normand, K. Raghavachari, A. Rendell, J. C. Burant, S. S. Iyengar, J. Tomasi, M. Cossi, N. Rega, N. J. Millam, M. Klene, J. E. Knox, J. B. Cross, V. Bakken, C. Adamo, J. Jaramillo, R. Gomperts, R. E. Stratmann, O. Yazyev, A. J. Austin, R. Cammi, C. Pomelli, J. W. Ochterski, R. L. Martin, K. Morokuma, V. G. Zakrzewski, G. A. Voth, P. Salvador, J. J. Dannenberg, S. Dapprich, A. D. Daniels, Ö. Farkas, J. B. Foresman, J. V. Ortiz, J. Cioslowski and D. J. Fox, *GAUSSIAN 09 (Revision A.02 SMP)*, Gaussian, Inc., Wallingford CT, 2009.
20 HyperChem(TM) Professional 8.0, http://www.hyper.com/ (assessed February, 2011), Hypercube, Inc., 1115 NW 4th Street, Gainesville, Florida 32601, USA.
21 X. Kong, PhD thesis, King's College London, University of London, 2008.
22 Z. D. Liu, H. H. Khodr, D. Y. Liu, S. L. Lu and R. C. Hider, *J. Med. Chem.*, 1999, **42**, 4814–4823.
23 Y. Ma, S. Roy, X. Kong, Y. Chen, D. Liu and R. C. Hider, *J. Med. Chem.*, 2012, **55**, 2185–2195.
24 S. Piyamongkol, Y. M. Ma, X. L. Kong, Z. D. Liu, M. D. Aytemir, D. van der Helm and R. C. Hider, *Chem.–Eur. J.*, 2010, **16**, 6374–6381.
25 B. L. Rai, L. S. Dekhordi, H. Khodr, Y. Jin, Z. Liu and R. C. Hider, *J. Med. Chem.*, 1998, **41**, 3347–3359.
26 R. C. Hider and A. D. Hall, *Prog. Med. Chem.*, 1991, **28**, 41–173.